Structural characterization and immunostimulatory activity of a glucan from natural *Cordyceps sinensis*

Junqiao Wang [a], Shaoping Nie [a*], Steve W. Cui [a,b], Zhijun Wang [a], Aled O. Phillips [c], Glyn O. Phillips [d], Yajing Li [e], Mingyong Xie [a*]

[a] *State Key Laboratory of Food Science and Technology, Nanchang University, 235 Nanjing East Road, Nanchang, Jiangxi Province, 330047, China*

[b] *Guelph Food Research Centre, Agriculture and Agri-Food Canada, 93 Stone Road West, Guelph, Ontario, N1G 5C9, Canada*

[c] *School of Medicine, University of Cardiff, Wales, UK*

[d] *Phillips Hydrocolloids Research Centre, Glyndwr University, Wrexham, LL11 2AW Wales, UK*

[e] *Qinghai Ta Er Sheng Gu Agricultural Science and Technology Co. Ltd., Xining 810003, China*

* Corresponding authors:

spnie@ncu.edu.cn (Professor Shaoping Nie, PhD), Tel. & Fax: +86-791-88304452.

myxie@ncu.edu.cn (Professor Mingyong Xie, PhD), Tel. & Fax: +86-791-83969009.

Abstract

A water-soluble polysaccharide, named NCSP-50, was obtained from natural *Cordyceps sinensis* by hot water extraction and ethanol fractionation precipitation. It was eluted as a single symmetrical peak and had an average molecular weight of 9.76×10^5 Da. The structure was determined by monosaccharide composition, methylation analysis, 1D/2D NMR spectroscopy, and enzymatic hydrolysis and characterization of the oligosaccharides by MALDI-TOF mass spectrometry. The repeating unit of this polysaccharide was proposed as follows:

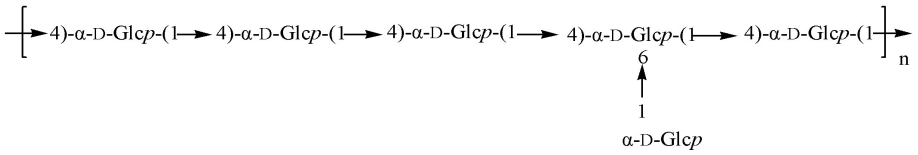

This glucan showed potent immunostimulatory activity on the basis of its significant abilities to promote macrophage proliferation, enhance NO production, as well as and cytokines (IL-1β and TNF-α) secretion.

Keywords: natural *Cordyceps sinensis*; α-glucan; caterpillar fungus; immunostimulatory

38 **1. Introduction**

39 *Cordyceps sinensis* (Berk.) Sacc. is a parasitic fungus growing on the larva of the caterpillar,
40 which was also called "Dong-Chong-Xia-Cao" in Chinese. As a famous traditional Chinese
41 medicine, *C. sinensis* has a long history being used as food/medicine, especially in "lung
42 protectorate" and "kidney improvement", as well as "Yin/Yang double invigorant" (Zhu, Halpern,
43 & Jones, 1998a, 1998b). In China, it was mainly distributed at Qinghai, Tibet, Sichuan, Yunnan
44 and Gansu plateau, at the elevation of 3500-5000 metres in the prairie soil. The growth of natural
45 *C. sinensis* needs a restricted habitat, so the yield is limited each year. But the production is
46 decreasing gradually during the recent years because of serious damage to ecological environment
47 and reckless harvesting. The demand of the market, on the contrary, experiences a constant
48 increase owing to a raising awareness of its multi-biological properties to the public. The
49 pharmacological effect of *C. sinensis* might be attributed to its chemical constituents and bioactive
50 ingredients, including polysaccharides, amino acids, minerals, nucleosides, cordycepic acid,
51 cordycepin, *etc*. (Wang, et al., 2015). Among them, polysaccharides, which account for 3-8% of
52 the total dry weight (Zhao, Xie, Wang, & Li, 2014), have been demonstrated to exhibit a wide
53 range of bioactivities, such as antioxidant (Li, Li, Dong, & Tsim, 2001), anti-tumor (Chen, Shiao,
54 Lee, & Wang, 1997), liver and kidney protection (Liu, Zuo, Tao, & Liu, 2013; Wang, et al., 2014;
55 Wang, et al., 2010), anti-fibrosis (Yao, et al., 2014) and immunomodulatory effect (Nie, Cui, Xie,
56 Phillips, & Phillips, 2013; Sheng, Chen, Li, & Zhang, 2011; Wu, et al., 2014). In our previous
57 study, a hydrophilic polysaccharide fraction (CBHP) mainly made up of glucose (95.15%) from
58 cultured *C. sinensis* was demonstrated to exhibit potent antifibrotic effect against renal fibrosis
59 (Nie et al., 2011; Zhang, Liu, Al-Assaf, Phillips, & Phillips, 2012).

60 Besides, *in vivo* and *in vitro* immuomodulating properties of polysaccharide from cultured *C.*
61 *sinensis* have been also well documented over the past decades. UM01 PS, a polysaccharide from
62 mycelia of *C. sinensis* fungus UM01, could significantly promote cell proliferation, phagocytic
63 ability, NO release, as well as multiply cytokines and chemokine production in macrophages
64 (Meng, et al., 2014). Cordysinocan, an exopolysaccharide from cultured *Cordyceps* UST 2000,
65 showed a stimulating effect on the human T-lymphocytes was demonstrated as well (Cheung, *et*
66 *al.*, 2009). Zhang *et al.* reported that the polysaccharide could enhance the immunity of ^{60}Co
67 radiation-induced immunosuppression mice through reducing oxidative injury and modulating
68 cytokine production (Zhang, *et al.*, 2011). It was evidenced that these polysaccharides with
69 effective immunodulating activity was mainly made up of galactose, glucose and mannose.
70 However, there are few reports demonstrating such effect of polysaccharides from natural
71 occurring *C. sinensis* at present. Additionally, significant differences in terms of chemical
72 composition and molecular weight of water-extracted polysaccharides between natural *C. sinensis*
73 and the cultured mycelium have been observed in our recent study (Wang *et al*., accepted).
74 Therefore, in this study, we aimed to characterize the detailed chemical structure of a glucan from
75 natural *C. sinensis* using methylation analysis, enzymatic hydrolysis, MALDI-TOF and 1D/2D
76 NMR spectroscopy, and further evaluate the immunostimulatory effect with regard to cell
77 proliferation assay, production of NO and cytokines in RAW 264.7 cells. This work will provide
78 useful information on the advanced structural characteristics of the polysaccharides from *C.*
79 *sinensis*, and will be helpful for further studying the structure and activity relationship.

80 **2. Materials and methods**

81 2.1 Materials

82 Natural *C. sinensis* was sampled from Qinghai province, China. T-series dextrans (T-10, T-40,
83 T-70, T-500 and T-2000) were purchased from Pharmacia Biotech (Uppsala, Sweden) and
84 monosaccharide standards (fucose, rhamnose, arabinose, galactose, glucose, mannose, xylose,
85 fructose, ribose, galacturonic acid and glucuronic acid), lipopolysaccharide (LPS) and super DHB
86 were from Sigma-Aldrich (St. Louis, MO, USA). Deuterium oxide (D_2O) and sodium
87 borodeuteride ($NaBD_4$, 98 atom% D) were from Acros Organics (New Jersey, USA). α-amylase
88 was purchased from Megazyme (Wicklow, Ireland) and HPLC grade methanol was from Merk
89 (Darmstadt, Germany). All other reagents were of analytical grade unless specified.

90 2.2 Isolation and purification

91 The natural *C. sinensis* was grounded and defatted with 80% ethanol overnight. Subsequently, the
92 dried ethanol-insoluble residues were extracted three times with distilled water (1:20, w/v) at 95˚C,
93 2 h each time. After centrifugation, all the supernatant was concentrated and precipitated with
94 ethanol until reaching a final concentration of 80%. The resulting precipitate was collected by
95 centrifugation and lyophilization, giving the crude polysaccharide. It was then removed protein by
96 Sevag reagent (chloroform/1-butanol, v/v = 4:1), resulting a white polysaccharide named as
97 NCSP.

98 NCSP was then purified by a stepwise fractionated precipitation with ethanol. Specifically,
99 anhydrous ethanol was added slowly to the polysaccharide solution (5 mg/mL) until the final
100 concentration of ethanol reached 30%. The solution was then kept stationary overnight, followed
101 by centrifugation at 4800 rpm for 20 min. The precipitate was collect and repeatedly washed with
102 anhydrous ethanol three times. The supernatant, on the other hand, was subjected to the next step
103 of precipitation with a higher ethanol concentration. In this way, the precipitated fractions were

104 obtained successively at final ethanol concentration of 30%, 50% and 70%, designated as
105 NCSP-30, NCSP-50 and NCSP-70, respectively. The final supernatant fraction, namely
106 NCSP-S70, was also collected.

107 2.3 Assay for structural analysis

108 2.3.1 Homogeneity and molecular weight determination

109 The homogeneity and molecular weight distribution of polysaccharide fractions were determined
110 by HPGPC on an Agilent 1260 LC instrument equipped with a refractive index detector (RID), a
111 variable wavelength detector (VWD), coupled with an Ultrahydrogel^{TM} 1000 column (7.8 mm ×
112 300 mm, Waters, USA) and an Ultrahydrogel^{TM} Linear column (7.8 mm × 300 mm, Waters, USA).
113 Polysaccharide solution was filtered through 0.45 μm filter prior to injection, with 0.1 M
114 NaCl/0.02% NaN_3 aqueous solution as mobile phase at a flow rate of 0.6 mL/min. The molecular
115 weight of polysaccharides was estimated using a standard curve prepared by T-series dextrans.
116 According to the information obtained from HPGPC that would be discussed later in this study,
117 we selected NCSP-50 for the following analysis.

118 2.3.2 Monosaccharide composition analysis

119 The identification and quantification of monosaccharide composition of NCSP-50 was achieved
120 by high performance anion exchange chromatography coupled with pulsed amperometric
121 detection (HPAEC-PAD) (Dionex ICS-5000 System, Dionex Corporation, CA). NCSP-50 (5 mg)
122 were dissolved in 0.5 mL 12M H_2SO_4 at an ice bath for 30 min, and then diluted to 3 mL (2 M
123 H_2SO_4) to further hydrolysis 2 h at 100˚C. Separation was performed on a CarboPac PA20 column
124 (3 mm×150 mm, Dionex, CA) and a CarboPac PA20 Guard (3 mm × 30 mm, Dionex, CA) with a
125 gradient elution procedure at a flow rate of 0.5 mL/min at 30˚C. The eluents consisted of 250 mM

126 NaOH solution (A), distilled water (B) and 1M sodium acetate (C). Initially, 0.8% A was eluted
127 for 20 min, and then a gradient increase from 5% C to 20% C while maintaining 0.8% A. Finally,
128 80% A was eluted to regenerate the column for 20 min. Chromeleon software was used to process
129 the data.

130 2.3.3 Methylation analysis

131 Methylation analysis was carried out according to the method of Ciucanu and Kerek (1984) with
132 slight modification. Briefly, dried NCSP-50 was completely dissolved in anhydrous DMSO and
133 then added dried NaOH powder to the solution with further stirring for 3 h. Iodomethane was
134 added to react with the solution in order to get the methlylated polysaccharide. A complete
135 methylation was confirmed by the disappearance of O-H absorption (3200-3700 cm^{-1}) in IR
136 spectrum. The methylated polysaccharide was hydrolyzed, reduced and acetylated to produce
137 partial methylated alditol acetates (PMAAs). Finally, the PMAAs were analyzed by GC-MS
138 (Agilent Technology 7890A/5975C, USA), equipped with a SP-2330 capillary column (30 m ×
139 0.25 mm, 0.2 mm film thickness, Supelco, Bellefonte, Pa). The GC temperature program was
140 isothermal at 160˚C, followed by 2 ˚C/min gradient up to 210˚C and 5 ˚C /min up to 240 ˚C. The
141 individual peaks of the PMAAs were identified by their characteristic GC retention times
142 (Biermann & McGinnis, 1988) and fragmentation patterns, as well as by comparison with mass
143 spectrum patterns from literature (Sassaki, Gorin, Souza, Czelusniak, & Iacomini, 2005).

144 2.3.4 NMR spectroscopy

145 NCSP-50 (30 mg) was dissolved in D_2O and then freeze dried. This procedure was repeated two
146 times to completely exchange H_2O with D_2O, and polysaccharide was finally dissolved in 1 mL
147 D_2O at room temperature for 3h before NMR analysis. Both ^{1}H and ^{13}C spectrum were recorded

148 on a Bruker Avance 600 MHz NMR spectrometer (Brucker, Rheinstetten, Germany) at 294 K.
149 NCSP-50 was further subjected to 2D NMR spectroscopy, including homonuclear $^{1}H/^{1}H$
150 correlation (COSY, TOCSY), heteronuclear single-quantum coherence (HSQC) and heteronuclear
151 multiple-bond correlation (HMBC) experiments through the standard Bruker pulse sequence.

152 2.3.5 Enzymatic hydrolysis and matrix-assisted laser desorption/ionization time-of-flight
153 (MALDI-TOF) analysis

154 NCSP-50 (5mg) was dissolved in 5 mL distilled water and digested for 36 h at 37°C with 100 μL
155 of α-Amylase (EC3.1.1.1 from *Bacillus amyloliquefaciens*). The enzymatic reaction was
156 terminated by heating the solution at 100°C for 15 min. This solution was injected into HPLC to
157 obtain the profile of molecular weight distribution after enzyme digestion. On the other hand, the
158 solution was precipitated with four volumes of anhydrous ethanol and then centrifuged. The
159 resulting precipitation was collected and lyophilized to harvest a mixture of oligosaccharide
160 named NCSP-50-E. NCSP-50-E was dissolved in water and further analyzed by MALDI-TOF.
161 For MALDI-TOF analysis, mass spectrum was recorded on an AB SCIEX TOF/TOF™ 5800
162 System (Framingham, MA 01701, USA) equipped with nitrogen laser operating at 337 nm. Super
163 DHB was used as the matrix at a concentration of 10 mg/mL dissolved in 0.1% Trifluoroacetic
164 acid (TFA) 50% methanol-water solution. NCSP-50-E (10μL) was mixed with 10 μL of the matrix
165 solution and a total of 1 μL of this mixture was applied to a stainless steel plate and allowed to dry
166 under vacuum at room temperature. Spectra were acquired both in the linear and reflector mode.

167 2.4 Immunostimulatory activity *in vitro*

168 2.4.1 Cell culture

169 Murine macrophage cell line RAW 264.7 (Shanghai Institute of Cell Biology, Shanghai, China)

170 was cultured in RPMI 1640 medium containing 10% fetal bovine serum (FBS) and 100 U/mL
171 penicillin and 100 μg/mL streptomycin under a humidified incubator (37˚C, 5% CO_2).

172 2.4.2 Macrophage proliferation assay

173 The effect of NCSP-50 on the viability of RAW 264.7 cells was determined by a WST-8 Cell
174 Counting Kit-8 (Beyotime Biotechnology, Jiangsu, China). The cells (100 μL) were seeded into a
175 96-well plate at a density of 1.0×10^5 cells/mL and incubated for 4 h at 37˚C in a humidified
176 incubator with 5% CO_2. Subsequently, 100 μL RPMI 1640 medium in the presence of
177 polysaccharide solutions was added to each well reaching a final concentration of 0, 25, 50, 100
178 and 200 μg/mL and incubated for 24 h. LPS (1 μg/mL) was used as the positive control, RPMI
179 1640 medium in the absence of polysaccharide and LPS was used as the normal control, and
180 RPMI 1640 medium without cells was used as blank. At the end of incubation, CCK-8 solution
181 (10 μL) was added to each well and the plate was further incubated for 2 h. Absorbance was
182 recorded at 450 nm on the microplate reader (Varioskan Flash, Thermo Fisher Scientific, USA).

183 2.4.3 Nitric oxide (NO) production

184 The RAW 264.7 cells were suspended in the RPMI 1640 medium and adjusted to a density of 5.0
185 $\times 10^5$ cell/mL, followed by pipetting into 24-well plate in a volume of 1 mL. After pre-incubation
186 for 4 h, different concentrations of NCSP-50 or starch (0, 25, 50, 100 and 200 μg/mL), as well as
187 LPS (1 μg/mL) were treated for another 24 h. Afterwards, the conditioned medium was collected
188 and analyzed using a commercial-available NO assay kit (Beyotime Biotechnology, Jiangsu,
189 China) according to the manufacturer's protocol.

190 2.4.4 Cytokine secretion

191 For cytokine determination, RAW 264.7 cells (5.0×10^5 cells/well) were cultured in the presence

192 of different concentrations of polysaccharides (0, 25, 50, 100 and 200 μg/mL) and LPS (1 μg/mL)
193 for 24 h, and the culture supernatant was collected to determine the concentrations of various
194 cytokines (IL-1β and TNF-α) by ELISA kits (Boster Bio-engineering Limited Company, Wuhan,
195 China) according to the manufacturer's instruction.

196 2.5 Statistical analysis

197 All data was expressed as the mean ± standard deviation (SD). Comparison of the data was
198 conducted using one-way analysis of variance (ANOVA) followed by the Student-Newman-Keuls
199 test. A value of $P<0.05$ was considered to be statistically significant. All statistical analysis was
200 performed through statistical software (SPSS, Version 17.0).

201 **3. Results and discussion**

202 3.1 Isolation, purification and composition of NCSP-50

203 A crude polysaccharide (NCSP) from natural *C. sinensis* was obtained by hot water extraction and
204 ethanol precipitation, followed by removing protein, with a yield of 2.60% (w/w). After stepwise
205 ethanol precipitation, the subsequent yields of NCSP-30, NCSP-50, NCSP-70 and NCSP-S70
206 were 11.82%, 45.39%, 13.69% and 17.72% (w/w), respectively. The molecular weight distribution
207 of these four fractions was showed in Fig. 1A. NCSP-50, the major fraction obtained from NCSP,
208 exhibited only one symmetrical peak in HPGPC (Fig. 1A), indicating that the polysaccharide was
209 homogeneous. The other three fractions, however, should be processed for further purification
210 before structural identification. Therefore, we targeted NCSP-50 for the following analysis in this
211 study. The molecular weight of NCSP-50 was estimated to be 9.76×10^5 Da based on a calibration
212 curve prepared with standard dextrans. In addition, a small absorption at 280 nm was observed as
213 revealed by UV detector (Fig. 1B), with the retention time similar to that of the signal obtained for

214 NCSP-50 in RI detector, indicating that the small amount of protein may be conjugated with
215 NCSP-50. Monosaccharide composition analysis revealed that NCSP-50 consisted of only glucose
216 and no uronic acid was found. These results suggested that NCSP-50 was a highly purified,
217 water-soluble neutral glucan. However, in the previous reports, several studies had reported the
218 presence of glucose, galactose and mannose in the polysaccharides from *C. sinensis*. Miyazaki,
219 Oikawa, and Yamada (1977) revealed that the polysaccharide from ascocarps of *C. sinensis* was
220 composed of galactose and mannose with a molar ratio of 1:1. Kiho, Tabata, Ukai, and Hara (1986)
221 also purified a galactomannan from a 5% sodium carbonate extract of *C. sinensis* with a molecular
222 weight of about 2.3 kDa and the molar ratio between mannose and galactose was 3:5. Wu *et al.*
223 (2014) pointed out that the polysaccharide of *C. sinensis* collected from Sichuan province was
224 mainly composed of mannose, galactose and glucose with a molar ratio of 4.4:3.8:1.0 and had a
225 molecular weight of 22.45 kDa determined by SEC-MALLS. But the molecular weight of the
226 PSCS fraction, a polysaccharide from *C. sinensis* produced in Qinghai province, was about 100
227 kDa (Chen, *et al.*, 1997). Nie *et al.* found that the CBHP, fractionated from water soluble extracts
228 from cultured *C. sinensis* through DIAION HP-20 resin, was mainly composed of glucose
229 (95.19%), along with trace amount of mannose (0.91%) and galactose (0.61%) (Nie *et al*., 2011).
230 It seemed that differences in extraction processes and the origins might result in the discrepancies
231 of monosaccharide composition and molecular weight.

232 3.2 Methylation analysis

233 Based on the analysis of PMAAs, the linkage patterns of NCSP-50 were summarized in Table 1.
234 The result showed the presence of three major derivatives, 1,5-O-Ac_2-2,3,4,6-Me_4-glucitol,
235 1,4,5-O-Ac_2-2,3,6-Me_4-glucitol and 1,4,5,6-O-Ac_2-2,3-Me_2-glucitol, in a molar ratio of nearly

236 1:4:1, suggesting that NCSP-50 was an O-6-branched (1→4)-D-glucan.

237 3.3 ^{1}H NMR, ^{13}C NMR and 2D NMR

238 The ^{1}H NMR spectrum of the polysaccharide NCSP-50 exhibited three anomeric proton signals at
239 δ5.27, δ5.23 and δ 4.85 ppm, and labeled as A, B and C, respectively, according to their
240 decreasing chemical shifts (Fig. 2A). Based on ^{13}C NMR spectrum (Fig. 2B) and the cross peaks
241 in the HSQC spectrum (Fig. 2E), the anomeric carbon signal at 100.10 ppm (overlapped) was
242 correlated to both the anomeric proton signals at 5.27 and 5.23 ppm, and the anomeric carbon
243 signal at 99.01 ppm was correlated to the anomeric proton signal at 4.85 ppm. The chemical shifts
244 of anomeric proton and carbon signals indicated that all the three residues were presented in
245 α-configuration. All the ^{1}H and ^{13}C chemical shifts (Table 2) were completely assigned using
246 COSY, TOCSY, HSQC and HMBC experiments.

247 There was a high degree of signal overlapping between residue A and residue B in TOCSY
248 spectrum. This issue, however, was addressed by examining the well-resolved cross peaks in
249 COSY spectrum. The proton chemical shifts of residue A obtained were δ 5.27, 3.48, 3.82, 3.53
250 and 3.70 ppm for H-1, H-2, H-3, H-4 and H-5, respectively, from COSY spectrum (Fig. 2D and
251 Table 2). The chemical shifts of H-6/6' (δ 3.65 and 3.73 ppm) and C-6 (δ 60.85 ppm), on the other
252 hand, were confirmed by HSQC spectrum (Fig. 2E). The corresponding chemical shifts of the
253 other carbon, also revealed by HSQC spectrum, were 100.09, 72.01, 73.51, 77.28 and 71.52 ppm
254 for C-1, C-2, C-3, C-4 and C-5, respectively (Fig. 2E and Table 2). Theses assignments were also
255 supported by previous reports (Niu, Yan, Lv, Yao, & Yu, 2013; Petersen, Motawie, Møller,
256 Hindsgaul, & Meier, 2015; Shan, et al., 2014). The downfield shift of C-4 (77.28 ppm) confirmed
257 that residue A was →4)-α-D-Glc*p*-(1→.

258 Likewise, for residue B, the chemical shifts from H-1 to H-5 were assigned from COSY spectrum
259 (δ 5.23, 3.45, 3.56, 3.52 and 3.63 ppm) (Fig. 2D) and part of these was confirmed by TOCSY
260 spectrum (Fig. 2C and Table 2). Based on the proton chemical shifts, ^{13}C chemical shifts obtained
261 by HSQC spectrum were 100.09, 72.11, 73.22, 77.28 and 72.91 ppm, respectively (Fig. 2E).
262 According to the results from methylation analysis (Table 1), along with the literature data (Patra,
263 et al., 2013), the residue B was assigned to →4,6)-α-D-Glc*p*-(1→.
264 In the case of residue C, the chemical shifts of H-1, H-2, H-3, H-4 and H-5 was successfully
265 obtained from the COSY (Fig. 2D), which was 4.85, 3.43, 3.61, 3.29 and 3.59 ppm, respectively.
266 The specific allocation of H-6/6' chemical shifts were supported by HSQC spectrum (Fig. 2E).
267 According to TOCSY spectrum (Fig. 2C), only cross peaks of H-1/H-2 and H-2/H-3 were
268 available due to the weak correlation between the adjacent protons. All the ^{13}C chemical shifts of
269 residue C were achieved from HSQC spectrum (Fig. 2E). Comparison of proton and carbon
270 chemical shifts with the literature values (Petersen, et al., 2015; C. Zhao, Li, Luo, & Wu, 2006)
271 allowed assigning residue C to α-D-Glc*p*-(1→.
272 The HMBC experiment was carried out to enable us to identify glycosidic linkages between sugar
273 residues, as shown in Fig. 2F. Examining the cross peaks of both anomeric ^{1}H and ^{13}C of each
274 sugar residue could help to identify the sequence of residues in the polysaccharide. Cross peak
275 between H-1 (5.27 ppm) of residue A and C-4 (77.28 ppm) of residue A; H-4 (3.53 ppm) of
276 residue A and C-1 (100.09 ppm) of residue A; H-1 (5.23 ppm) of residue B and C-4 (77.28 ppm)
277 of residue A were observed, indicating that →4)-α-D-Glc*p*-(1→ and →4,6)-α-D-Glc*p*-(1→ were
278 linked to each other through 1,4-O-glycosidic bonds as the main chain of the polysaccharide.
279 3.4 Enzymatic hydrolysis and MALDI-TOF analysis

280 In order to confirm the proposed chemical structure of NCSP-50, a specific enzymatic hydrolysis
281 procedure was performed. The enzymatic hydrolysate was investigated using HPLC so as to
282 monitor the changes of molecular weight distribution after treating with α-amylase. As is shown in
283 Fig. 3A, it was obvious to see that the molecular weight of NCSP-50 was significantly decreased,
284 suggesting that the polysaccharide was very sensitive to α-amylase. Then, we removed the
285 corresponding digests by precipitation with 80% ethanol followed by centrifugation to isolate the
286 polysaccharide, designated as NCSP-50-E. The MALDI-TOF profile of NCSP-50-E was shown in
287 Fig. 3B and 3C. The distance between the adjacent peaks was 162 mass units, corresponding to the
288 hexose residue in this polysaccharide. Pentose, such as arabinose, xylose, which has a
289 peak-to-peak mass difference of 132 Da, were not presented in this fraction, in agreement with the
290 aforementioned result. A maximum degree of polymerization of NCSP-50-E was 30 (m/z 4901),
291 indicating that NCSP-50 was successfully hydrolyzed by α-amylase. Therefore, the result proved
292 that (1→4)-linked α-D-Glc*p* existed in the backbone of NCSP-50.
293 The structure of NCSP-50 seems to be similar to that of pant reserve α-1,4-linked glucans.
294 However, the C-6 linked side chains in NCSP-50 were constituted by single α-glucose unit, on
295 every forth of the main chain. It seems that the structural feature of NCSP-50 was similar to that of
296 amylose which was also a kind of linear α-1,4-linked glucan. Moreover, it is acknowledged that
297 starch polysaccharides are hardly dissolved in cold water and have a high viscosity. NCSP-50, on
298 the contrary, was soluble in cold water displaying a milk white, transparent solution. The
299 discrepancies in physicochemical properties between NCSP-50 and amylose might be attributed to
300 their differences in structure characteristics.
301 In our previous study, the structure of CBHP has been characterized, which had a main chain of

302 (1→4)-linked α-D-Glc*p* together with small amount of (1→3)-linked α-D-Glc*p* and the branching
303 points were located at O-2 or O-6 with α-terminal-linked Glc*p* as side chain (Nie *et al.*, 2011).
304 Obviously, CBHP had higher degree of branching compared to NCSP-50. Another difference
305 between them was the small amount of (1→3)-linked α-D-Glc*p* residues presented in the main
306 chain of CBHP. We speculated that the differences of the raw material and extraction procedures
307 might account for the varieties of the chemical structure between the two polysaccharides.

308 3.5 Immunostimulatory activities on macrophages

309 3.5.1 Effect of NCSP-50 on macrophage proliferation

310 Macrophages are presented in virtually all tissues and have long been considered as an important
311 component of host defense against microbial invaders and malignancies (Dunn, Barke, Ewald, &
312 Simmons, 1987). Additionally, macrophages can respond not only to endogenous stimuli
313 generated by injury or infection, but also to signals produced by antigen-specific immune cells
314 (Mosser & Edwards, 2008). Therefore, to characterize the immunostimulatory effect of NCSP-50
315 in an *in vitro* macrophage cell model, we firstly investigated the influence of cells proliferation in
316 the presence of polysaccharide with various concentrations (Fig. 4A). After 24 h incubation with
317 the polysaccharide solutions (25, 50, 100 and 200 μg/mL), the proliferation rate of RAW 264.7
318 cells was determined by the WST-8 assay. As shown in Fig. 4A, NCSP-50 exhibited a significant
319 stimulatory effect on RAW 264.7 cells proliferation. In the concentration of 50-200 μg/mL, the
320 proliferation rates of polysaccharide-treated groups were significantly higher than that of the
321 positive control group ($p<0.01$).

322 3.5.2 Effect of NCSP-50 on NO production in macrophages

323 NO is reported to be associated with macrophages activation in the host defense against tumor

324 cells and microorganisms (Schepetkin & Quinn, 2006). In order to investigate the effects of
325 NCSP-50 on macrophage response, the NO production of RAW 264.7 cells was determined by
326 Griess assay. As is shown in Fig. 4B, the NO concentration of the culture supernatant was
327 significantly increased in a dose-dependent manner by treatment with NCSP-50 (25-200 μg/mL,
328 $P<0.01$). The level of NO reached 22.32 μmol/L after treatment by 50 μg/mL of NCSP-50, similar
329 to that of the positive control (LPS, 1 μg/mL). In addition, in order to figure out the difference
330 between NCSP-50 and starch, the effect of starch on NO production was also evaluated (Fig. 4C).
331 After 24 h incubation in the presence of various concentrations of starch, it was obviously to see
332 that the production of NO was not significantly enhanced as compared to the control group (0
333 μg/mL). The results demonstrated that starch, although had a similar α-1,4-glucan backbone
334 structure, showed no effect on upregulating NO secretion in RAW 264.7 cells.

335 3.5.3 Effect of NCSP-50 on IL-1β and TNF-α secretion in macrophages

336 Cytokines are intercellular signaling proteins or peptides with relatively low molecular weight that
337 are released by the cells altering either their own function (autocrine) or those of adjacent cells
338 (paracrine) (Haddad, 2002). They are important mediators involved in modulating immune
339 response and inflammatory reactions, particularly during infection and trauma. In addition to
340 regulating cells of the innate and adaptive immune system, cytokines affect cell proliferation,
341 differentiation and functions (Hopkins, 2003). IL-1β and TNF-α are two typical pro-inflammatory
342 cytokines, which can be secreted by activated macrophages with immunomodulatory properties. It
343 is of significance that TNF-α could stimulate the production of genotoxic molecules, such as NO
344 and reactive oxygen species that could lead to DNA damage and mutations (Hussain, Hofseth, &
345 Harris, 2003). In the present study, the stimulatory effect of NCSP-50 on the production of IL-1β

346 and TNF-α by RAW 264.7 cells was determined by ELISA. As shown in Fig. 4D and 4E,
347 NCSP-50 could significantly promote RAW 264.7 cells to release IL-1β and TNF-α. With respect
348 to IL-1β, it is obviously that NCSP-50 could increase the IL-1β production in a dose-dependent
349 manner. Compared with the control group, the IL-1β concentration was significantly increased by
350 NCSP-50 treatment (25 μg/mL, $p < 0.05$; 50, 100 and 200 μg/mL, $p < 0.01$) and reached up to
351 51.47 pg/mL at a concentration of 200 μg/mL, slightly lower than that induced by LPS (54.95
352 pg/mL). On the other hand, with regard to TNF-α secretion, NCSP-50 also showed a notable
353 promotion effect, with the highest level of 74905.42 pg/mL at a concentration of 100 μg/mL. In
354 contrast, the influence of starch on TNF-α production was not significant at all concentrations as
355 evident in Fig. 4F. These results indicated that NCSP-50 could remarkably promote the secretion
356 of cytokines in RAW 264.7 cells, whereas starch had no effect.
357 Therefore, it was confirmed that the potent immunostimulatory activity of NCSP-50 should be
358 caused and influenced by its structure characteristics, different from that of the starch. The
359 discrepancy might be attributed to the degree of substitution on the main chain, the length of side
360 chains and the conformation etc., between NCSP-50 and starch.

361 **4. Conclusion**

362 In the present study, the structure properties of a water-soluble polysaccharide NCSP-50 from
363 natural *C. sinensis* were elucidated. HPGPC results showed that the molecular weight of NCSP-50
364 was 9.76×10^5 Da. Using monosaccharide composition, methylation analysis, enzymatic hydrolysis,
365 MALDI-TOF analysis and NMR spectroscopy, the structure of NCSP-50 was deduced to be a
366 homogenous glucan, comprised a main chain of (1→4)-linked-α-D-Glc*p* with a single α-D-Glc*p*
367 branch substituted at C-6. Unlike starch, NCSP-50 was revealed to significantly stimulate the

368 proliferation of macrophages, promote nitric oxide production and enhance cytokine secretion.
369 Our results demonstrated that NCSP-50 had the potential to be an immunopotentiating agent, and
370 the in-deep research on the related mechanism, on the other hand, will be conducted in our future
371 work.

372 **Acknowledgment**

373 The financial support from the National Natural Science Foundation of China for Excellent Young
374 Scholars (31422042), the outstanding science and technology innovation team project in Jiangxi
375 Province (20133BCB24001), the Project of Science and Technology of Jiangxi Provincial
376 Education Department (KJLD13004) and Research Project of State Key Laboratory of Food
377 Science and Technology (SKLF-ZZB-201508, SKLF-ZZA-201611) is gratefully acknowledged.

378

379 **Reference**

380 Biermann, C. J., & McGinnis, G. D. (1988). *Analysis of Carbohydrates by GLC and MS*: CRC
381 Press.

382 Chen, Y. J., Shiao, M. S., Lee, S. S., & Wang, S.-Y. (1997). Effect of *Cordyceps sinensis* on the
383 proliferation and differentiation of human leukemic U937 cells. *Life Sciences, 60*(25),
384 2349-2359.

385 Cheung, J. K., Li, J., Cheung, A. W., Zhu, Y., Zheng, K. Y., Bi, C. W., et al. (2009). Cordysinocan,
386 a polysaccharide isolated from cultured *Cordyceps*, activates immune responses in
387 cultured T-lymphocytes and macrophages: Signaling cascade and induction of cytokines.
388 *Journal of Ethnopharmacology, 124*(1), 61-68.

389 Ciucanu, I., & Kerek, F. (1984). A simple and rapid method for the permethylation of

390 carbohydrates. *Carbohydrate Research, 131*(2), 209-217.

391 Dunn, D. L., Barke, R. A., Ewald, D. C., & Simmons, R. L. (1987). Macrophages and
392 translymphatic absorption represent the first line of host defense of the peritoneal cavity.
393 *Archives of Surgery, 122*(1), 105-110.

394 Haddad, J. J. (2002). Cytokines and related receptor-mediated signaling pathways. *Biochemical*
395 *and Biophysical Research Communications, 297*(4), 700-713.

396 Hopkins, S. J. (2003). The pathophysiological role of cytokines. *Legal Medicine, 5*, S45-S57.

397 Hussain, S. P., Hofseth, L. J., & Harris, C. C. (2003). Radical causes of cancer. *Nature Reviews*
398 *Cancer, 3*(4), 276-285.

399 Kiho, T., Tabata, H., Ukai, S., & Hara, C. (1986). A minor, protein-containing galactomannan from
400 a sodium carbonate extract of *Cordyceps sinensis*. *Carbohydrate Research, 156*, 189-197.

401 Li, S. P., Li, P., Dong, T. T. X., & Tsim, K. W. K. (2001). Anti-oxidation activity of different types
402 of natural *Cordyceps sinensis* and cultured *Cordyceps* mycelia. *Phytomedicine, 8*(3),
403 207-212.

404 Liu, Y., Zuo, J., Tao, Y., & Liu, W. (2013). Protective effect of *Cordyceps* polysaccharide on
405 hydrogen peroxide-induced mitochondrial dysfunction in HL-7702 cells. *Molecular*
406 *Medicine Reports, 7*(3), 747-754.

407 Meng, L.-Z., Feng, K., Wang, L.-Y., Cheong, K.-L., Nie, H., Zhao, J., et al. (2014). Activation of
408 mouse macrophages and dendritic cells induced by polysaccharides from a novel
409 *Cordyceps sinensis* fungus UM01. *Journal of Functional Foods, 9*, 242-253.

410 Miyazaki, T., Oikawa, N., & Yamada, H. (1977). Studies on fungal polysaccharides. XX.
411 Galactomannan of *Cordyceps sinensis*. *Chemical and Pharmaceutical Bulletin, 25*(12),

412 3324-3328.

413 Mosser, D. M., & Edwards, J. P. (2008). Exploring the full spectrum of macrophage activation.
414 *Nature Reviews Immunology, 8*(12), 958-969.

415 Nie, S. P., Cui, S. W., Phillips, A. O., Xie, M.-Y., Phillips, G. O., Al-Assaf, S., et al. (2011).
416 Elucidation of the structure of a bioactive hydrophilic polysaccharide from *Cordyceps*
417 *sinensis* by methylation analysis and NMR spectroscopy. *Carbohydrate Polymers, 84*(3),
418 894-899.

419 Nie, S., Cui, S. W., Xie, M., Phillips, A. O., & Phillips, G. O. (2013). Bioactive polysaccharides
420 from *Cordyceps sinensis*: Isolation, structure features and bioactivities. *Bioactive*
421 *Carbohydrates and Dietary Fibre, 1*(1), 38-52.

422 Niu, Y., Yan, W., Lv, J., Yao, W., & Yu, L. (2013). Characterization of a novel polysaccharide from
423 tetraploid *Gynostemma pentaphyllum* Makino. *Journal of Agricultural and Food*
424 *Chemistry, 61*(20), 4882-4889.

425 Patra, S., Patra, P., Maity, K. K., Mandal, S., Bhunia, S. K., Dey, B., et al. (2013). A heteroglycan
426 from the mycelia of *Pleurotus ostreatus*: Structure determination and study of antioxidant
427 properties. *Carbohydrate Research, 368*, 16-21.

428 Petersen, B. O., Motawie, M. S., Møller, B. L., Hindsgaul, O., & Meier, S. (2015). NMR
429 characterization of chemically synthesized branched α-dextrin model compounds.
430 *Carbohydrate Research, 403*, 149-156.

431 Sassaki, G. L., Gorin, P. A., Souza, L. M., Czelusniak, P. A., & Iacomini, M. (2005). Rapid
432 synthesis of partially O-methylated alditol acetate standards for GC–MS: Some relative
433 activities of hydroxyl groups of methyl glycopyranosides on Purdie methylation.

434 *Carbohydrate Research, 340*(4), 731-739.

435 Schepetkin, I. A., & Quinn, M. T. (2006). Botanical polysaccharides: macrophage
436 immunomodulation and therapeutic potential. *International Immunopharmacology, 6*(3),
437 317-333.

438 Shan, J., Sun, G., Ren, J., Zhu, T., Jia, P., Qu, W., et al. (2014). An α-glucan isolated from root of
439 *Isatis Indigotica*, its structure and adjuvant activity. *Glycoconjugate Journal, 31*(4),
440 317-326.

441 Sheng, L., Chen, J., Li, J., & Zhang, W. (2011). An exopolysaccharide from cultivated *Cordyceps*
442 *sinensis* and its effects on cytokine expressions of immunocytes. *Applied Biochemistry*
443 *and Biotechnology, 163*(5), 669-678.

444 Wang, J., Kan, L., Nie, S., Chen, H., Cui, S. W., Phillips, A. O., et al. (2015). A comparison of
445 chemical composition, bioactive components and antioxidant activity of natural and
446 cultured *Cordyceps sinensis*. *LWT-Food Science and Technology, 63*(1), 2-7.

447 Wang J., Nie S., Kan L., Chen H., Cui S., Phillips A. O., et al. Comparison of structural features
448 and antioxidant activity of polysaccharides from natural and cultured *Cordyceps sinensis*.
449 *Food Science and Biotechnology, Accepted*.

450 Wang, Y., Liu, D., Zhao, H., Jiang, H., Luo, C., Wang, M., et al. (2014). *Cordyceps sinensis*
451 polysaccharide CPS-2 protects human mesangial cells from PDGF-BB-induced
452 proliferation through the PDGF/ERK and TGF-β1/Smad pathways. *Molecular and*
453 *Cellular Endocrinology, 382*(2), 979-988.

454 Wang, Y., Yin, H., Lv, X., Wang, Y., Gao, H., & Wang, M. (2010). Protection of chronic renal
455 failure by a polysaccharide from *Cordyceps sinensis*. *Fitoterapia, 81*(5), 397-402.

456 Wu, D.T., Meng, L.Z., Wang, L.Y., Lv, G. P., Cheong, K. L., Hu, D. J., et al. (2014). Chain
457 conformation and immunomodulatory activity of a hyperbranched polysaccharide from
458 *Cordyceps sinensis*. *Carbohydrate Polymers, 110*, 405-414.
459 Yao, X., Meran, S., Fang, Y., Martin, J., Midgley, A., Pan, M.-M., et al. (2014). *Cordyceps sinensis*:
460 *In vitro* anti-fibrotic bioactivity of natural and cultured preparations. *Food Hydrocolloids,*
461 *35*, 444-452.
462 Zhang, J., Yu, Y., Zhang, Z., Ding, Y., Dai, X., & Li, Y. (2011). Effect of polysaccharide from
463 cultured *Cordyceps sinensis* on immune function and anti-oxidation activity of mice
464 exposed to ^{60}Co. *International Immunopharmacology, 11*(12), 2251-2257.
465 Zhang, X., Liu B., Al-Assaf, S., Phillips, G. O., & Phillips, A. O. (2012). *Cordyceps sinensis*
466 decreases TGF-β1 dependent epithelial to mesenchymal transdifferentiation and
467 attenuates renal fibrosis. *Food Hydrocolloids*, 28(1), 200-212.
468 Zhao, C., Li, M., Luo, Y., & Wu, W. (2006). Isolation and structural characterization of an
469 immunostimulating polysaccharide from fuzi, *Aconitum carmichaeli*. *Carbohydrate*
470 *Research, 341*(4), 485-491.
471 Zhao, J., Xie, J., Wang, L. Y., & Li, S. P. (2014). Advanced development in chemical analysis of
472 *Cordyceps*. *Journal of Pharmaceutical and Biomedical Analysis, 87*, 271-289.
473 Zhu, J.-S., Halpern, G. M., & Jones, K. (1998a). The scientific rediscovery of a precious ancient
474 Chinese herbal regimen: *Cordyceps sinensis* Part II. *The Journal of Alternative and*
475 *Complementary Medicine, 4*(4), 429-457.
476 Zhu, J.-S., Halpern, G. M., & Jones, K. (1998b). The scientific rediscovery of an ancient Chinese
477 herbal medicine: *Cordyceps sinensis* Part I. *The Journal of Alternative and*

478 *Complementary Medicine, 4*(3), 289-303.

479

480

481 **TABLES**

482 **Table 1**

483 GC-MS of alditol acetate derivatives from the methylated products of NCSP-50

Methylated sugar	RT(min)	Deduced linkage	Molar ratio [a]
1,5-O-Ac_2-2,3,4,6-Me_4-glucitol	15.333	D - Glc*p*-(1→	15.99
1,4,5-O-Ac_2-2,3,6-Me_3-glucitol	23.856	→4)- D -Glc*p*-(1→	66.87
1,4,5,6-O-Ac_2-2,3-Me_2-glucitol	29.311	→4,6)- D -Glc*p*-(1→	17.14

484 [a] Relative molar ratio, calculated from the ratio of peak areas.

485

486

487 **Table 2**

488 The ^{1}H NMR and ^{13}C NMR chemical shifts for NCSP-50 isolated from natural *Cordyceps sinensis*

489 in D_2O at 295K

		Chemical shifts (ppm)						
	Glycosidic linkage	H1/C1	H2/C2	H3/C3	H4/C4	H5/C5	H6/C6	
A	→4)-α-D-Glc*p*-(1→	5.27	3.48	3.82	3.53	3.70	3.73[a]	3.65[b]
		100.09	72.01	73.51	77.28	71.52	60.85	
B	→4,6)-α-D-Glc*p*-(1→	5.23	3.45	3.56	3.52	3.63	3.30	-
		100.09	72.11	73.22	77.28	72.91	69.73	
C	α-D-Glc*p*-(1→	4.85	3.43	3.61	3.29	3.59	3.72[a]	3.63[b]
		99.01	72.16	73.28	69.7	73.07	60.74	

490 [a,b] interchangeable

491

492

493

494 **FIGURES**

495 **Figure 1**

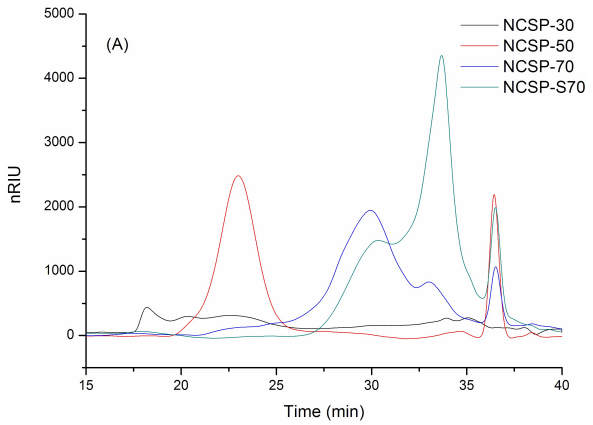

496

497

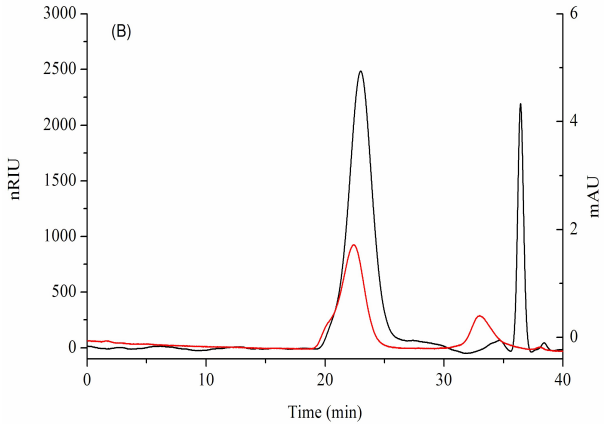

498

499

500

501

502

503

504

505

506

507 **Figure 2**

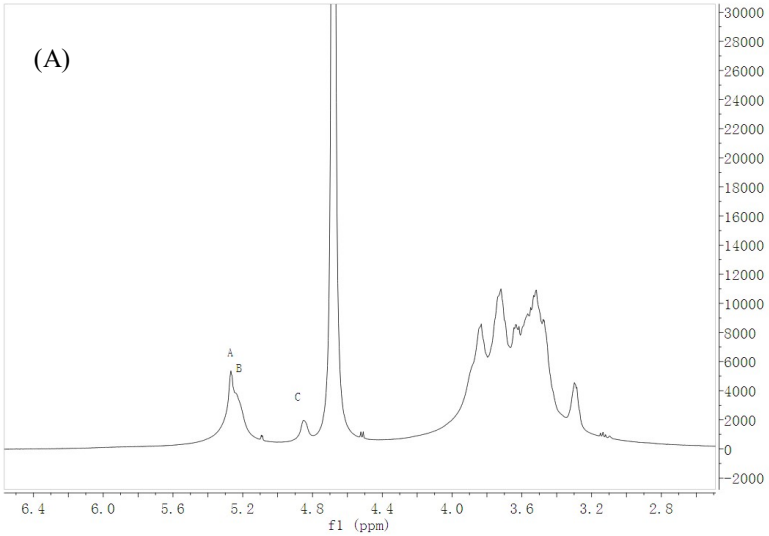

508

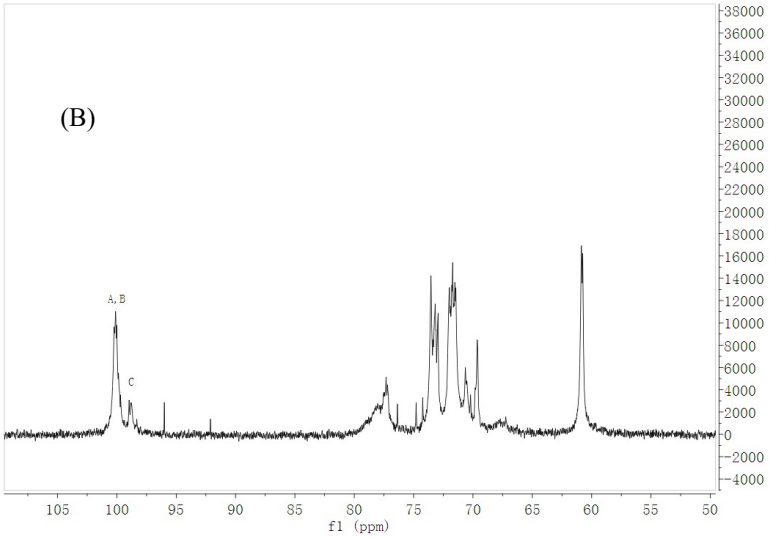

509

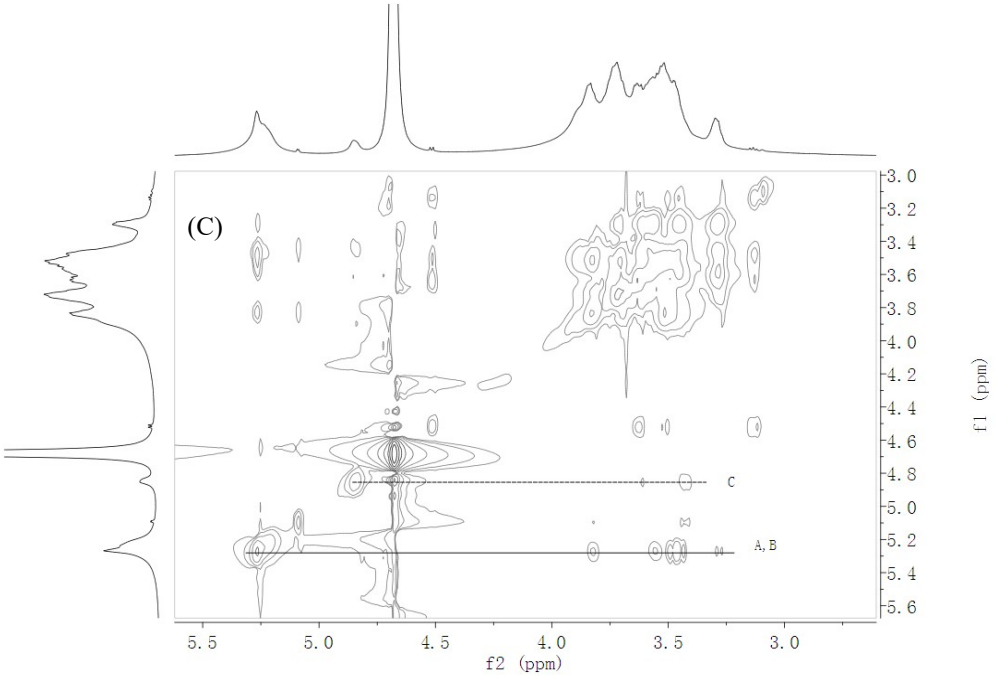
(C)
C
A, B
f2 (ppm)
f1 (ppm)

510

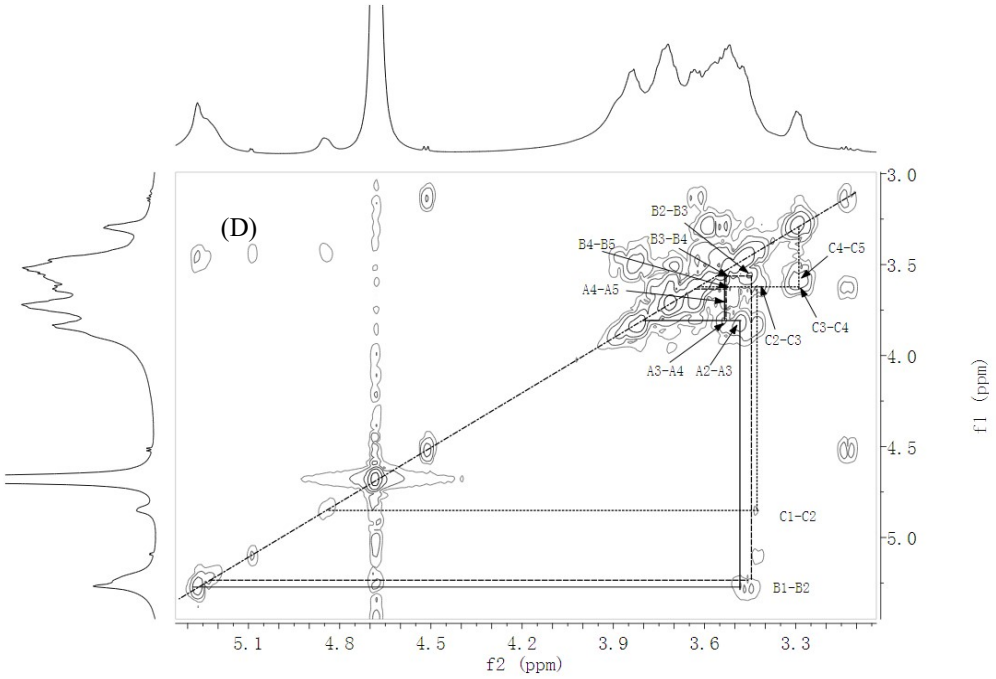
(D)
B2-B3
B3-B4
B4-B5
A4-A5
C4-C5
C3-C4
C2-C3
A3-A4
A2-A3
C1-C2
B1-B2
f2 (ppm)
f1 (ppm)

511

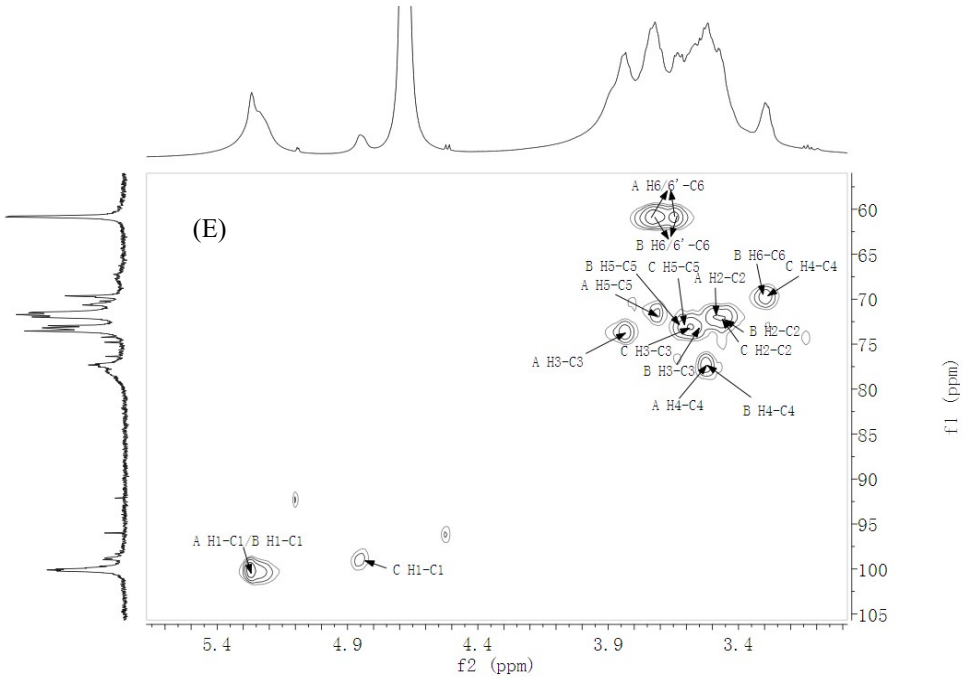

512

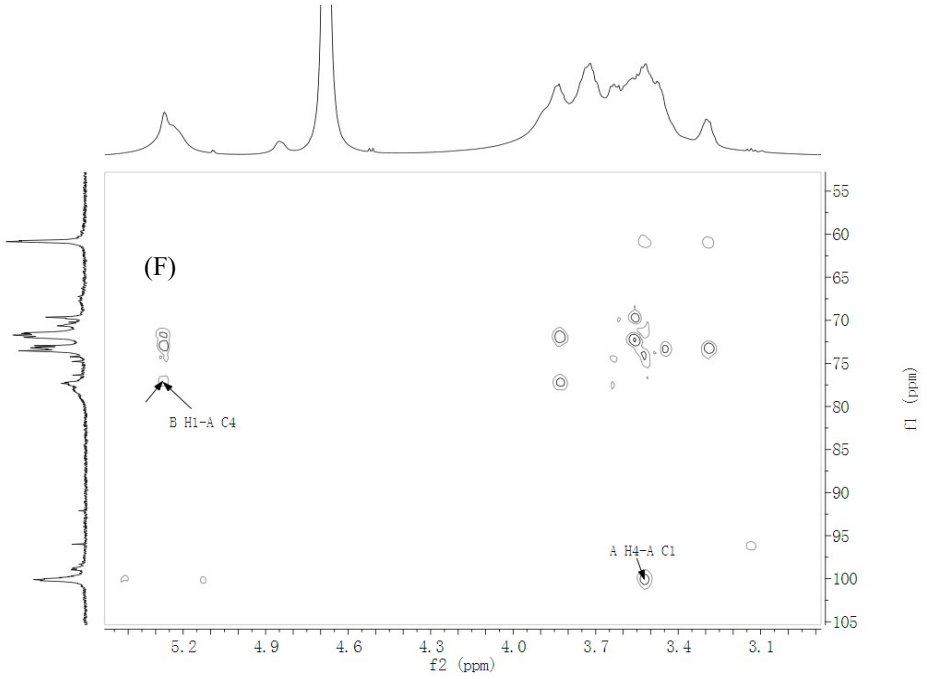

513

514

515

516

517

518 **Figure 3**

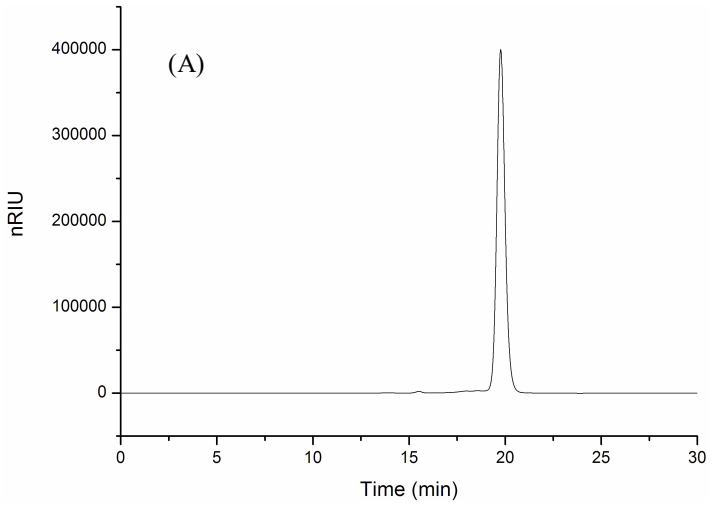

519

520

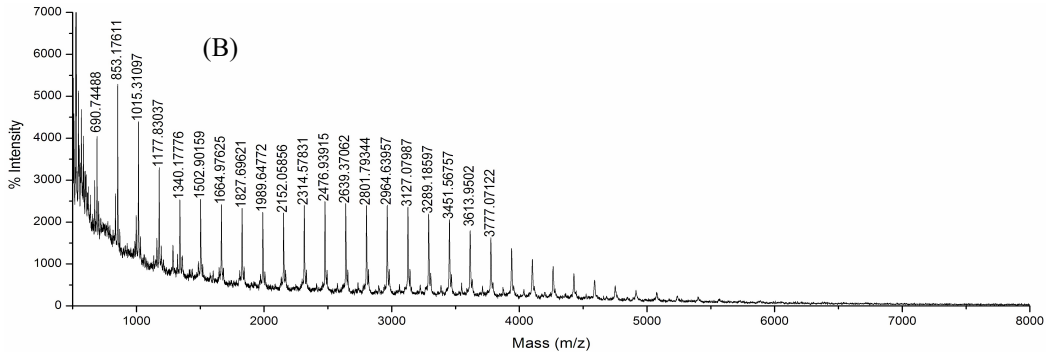

521

522

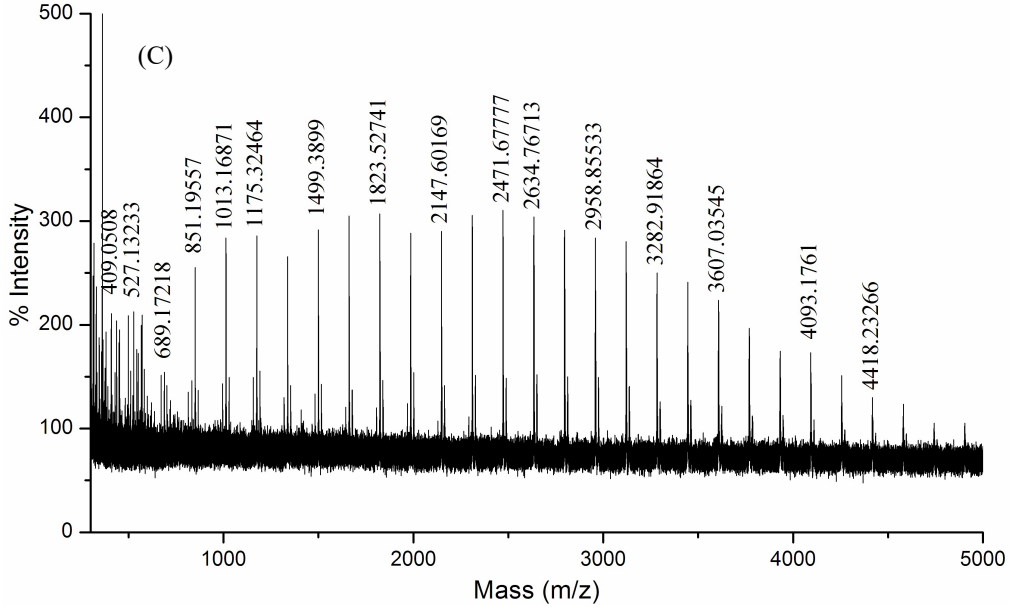

523

524 **Figure 4**

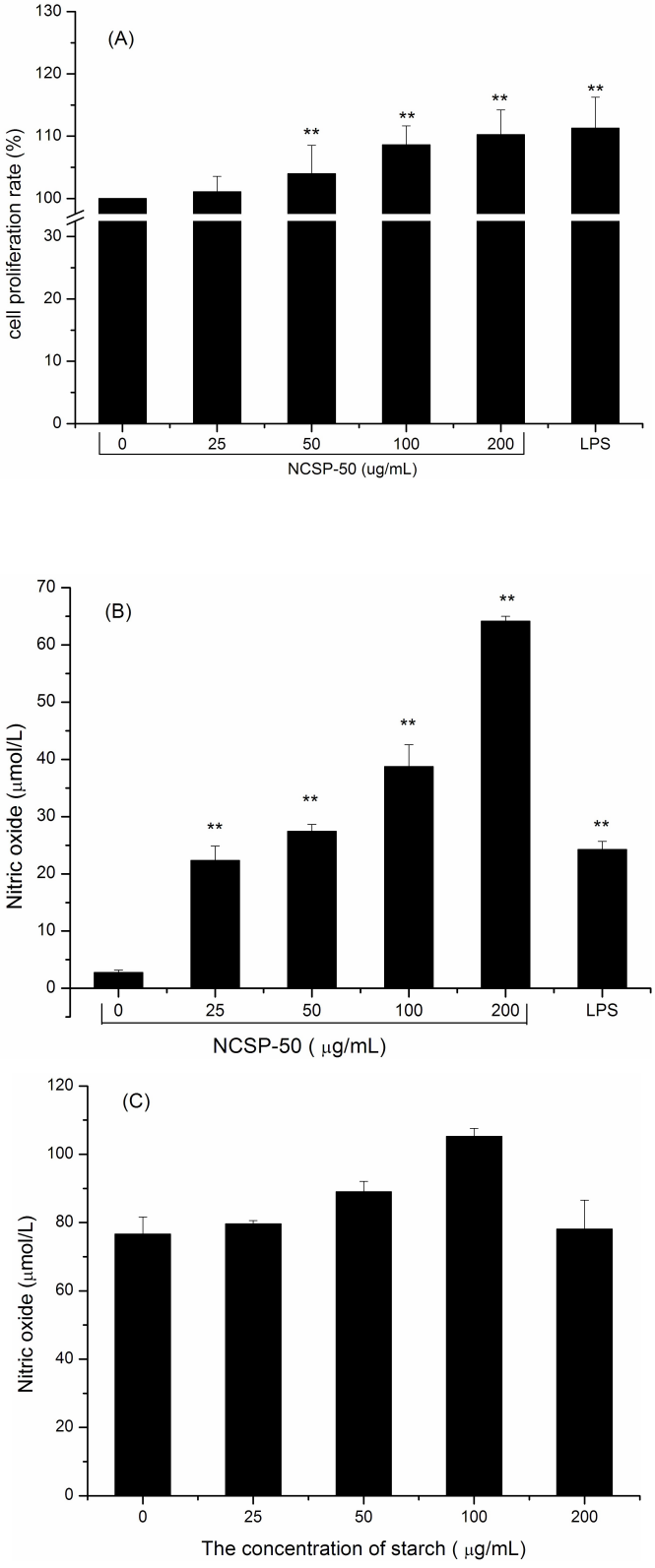

525

526

527

528

529

530

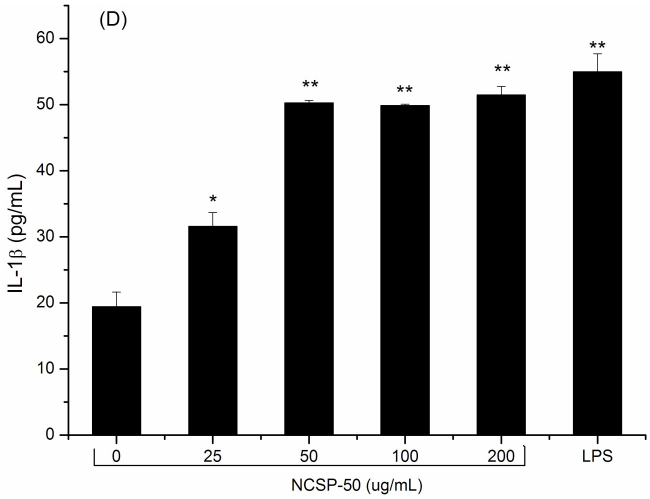

531

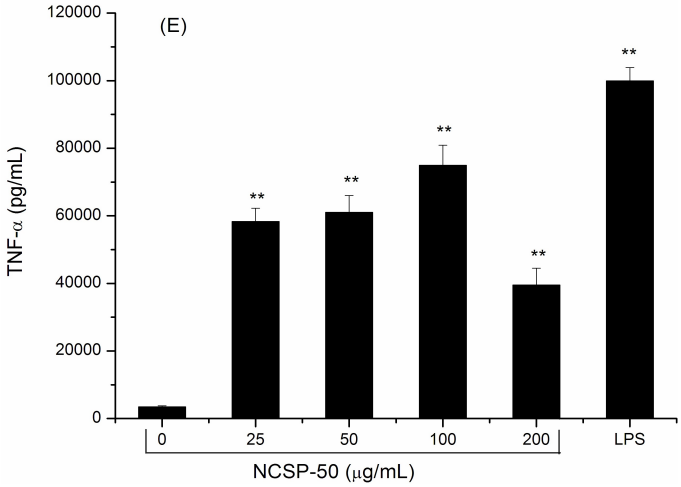

532

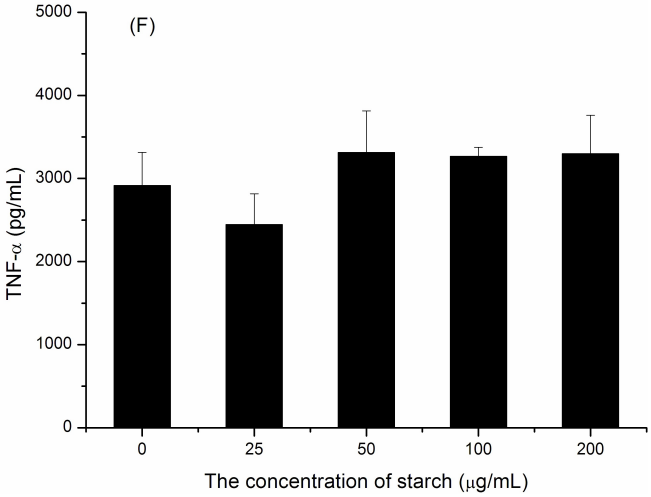

533

534